another phantom study with a 10-cm-diameter hollow phantom.

The CBF value in each ROI was calculated by numerically solving the equation (1) as reported previously (Temma *et al*, 2004).

$$R(t) = fA_W(t) * e^{-(f/p+\lambda)t} \quad (1)$$

where the asterisk denotes the convolution integral and other marks are the tissue concentration of ^{15}O radioactivity ($R(t)$), a typical example of that in the late phase experiment is presented in Figure 1, CBF (f), the arterial concentration of ^{15}O-water radioactivity ($A_W(t)$), partition coefficient of water between the brain and blood ($P = 0.8$) and physical decay constant of ^{15}O (λ).

Then, the OEF value was calculated using the same equation (Eq. 2) as that applied to the bolus inhalation of ^{15}O-O_2 gas method (Mintun *et al*, 1984; Shidahara *et al*, 2002), which could be used with this pharmaceutical as shown previously (Magata *et al*, 2003)

$$R(t) = \mathrm{OEF}fA_O(t) * e^{-(f/p+\lambda)t} + fA_W(t) * e^{-(f/p+\lambda)t} + V_B R(1 - V_V' \mathrm{OEF})A_O(t) \quad (2)$$

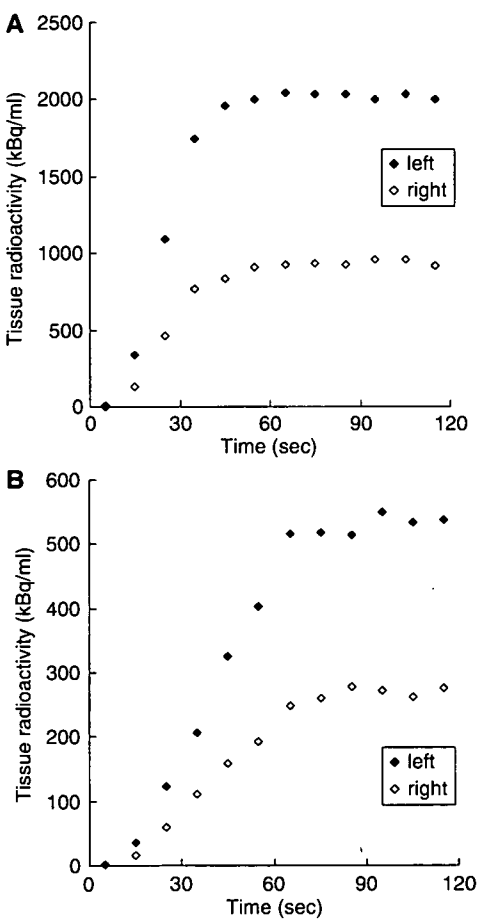

Figure 1 Typical curves of ^{15}O radioactivity obtained by the PET scanning using (**A**) ^{15}O-H_2O and (**B**) injectable ^{15}O-O_2 24 h after the right MCA occlusion.

where the arterial concentration of ^{15}O-O_2 radioactivity ($A_O(t)$), cerebral blood volume ($V_B = 0.04$ mL/g), the hematocrit ratio between central and peripheral regions ($R = 0.85$) and the effective venous ratio in the brain ($V_V' = 0.835$) are used.

The $CMRO_2$ value was calculated using equation (3). In this equation, Hb is gram hemoglobin/mL blood and %Sat is percent saturation of O_2 (Shidahara *et al*, 2002).

$$\mathrm{CMRO_2} = \frac{(1.39 \times \mathrm{Hb} \times \%\mathrm{Sat})}{100} \times \mathrm{OEF} \times \mathrm{CBF} \quad (3)$$

Results

Injectable ^{15}O-O_2 Labeling

The shape of an artificial lung was modified to increase ^{15}O labeling efficiency. Namely, the artificial lung used was three times longer (18 cm) than the previous version while the density of plastic fibers and diameter of the lung were unchanged (Magata *et al*, 2003). In this system, 90 MBq/ml was obtained at maximum.

Physiological Parameters

Blood gases were analyzed several times during the experiment (Table 1). Although several parameters were significantly changed, these changes were slight and levels were not in the abnormal range.

Studies at 1 h After Onset

The relationships between CBF, OEF and $CMRO_2$ at 1 h after the occlusion are shown in scatter diagrams (Figures 2 and 3). As revealed in Figure 2, in the right hemisphere, a decrease in CBF and compensatory increase in OEF were indicated in comparison with the opposite side, inducing a good reciprocal relationship as a whole. Also, the decrease in CBF in the right hemisphere was not so marked. Figure 3 shows the relationship between CBF and $CMRO_2$.

Table 1 Arterial blood gas values before and after PET experiments in MCA occlusion

	1 h		*24 h*	
	Before	*After*	*Before*	*After*
pH	7.32 (0.03)	7.33 (0.03)	7.36 (0.04)	7.35 (0.04)
PO_2 (mm Hg)	97.4 (5.7)	102.8 (10)	94.8 (7.4)	101.5 (4.3)*
PCO_2 (mm Hg)	44.3 (4.2)	39.8 (3.4)	39.7 (4.8)	36.9 (3.7)*
Hct (%)	54.4 (4.8)	51.5 (3.8)*	55 (3.3)	53.5 (3.1)
O_2Sat (%)	96.9 (0.4)	97.2 (0.8)	96.9 (0.7)	97.4 (0.3)*
Hb (g/dl)	18.5 (1.6)	17.5 (1.3)*	18.7 (1.2)	18.2 (1.0)

Statistical differences in each physiological parameter between before and after PET experiments were determined using the Wilcoxon signed-rank test; *$P < 0.05$.
Values listed are means (s.d.).

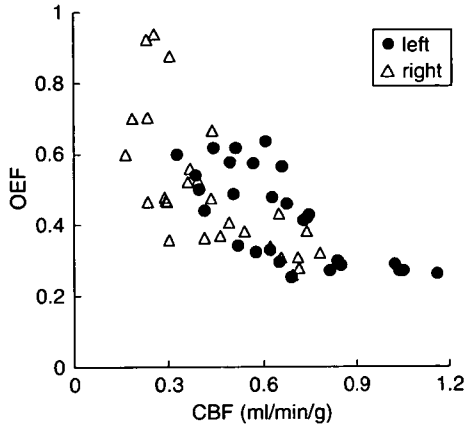

Figure 2 Scatter diagram of CBF (mL/min/g) and OEF values 1 h after the onset of MCA occlusion.

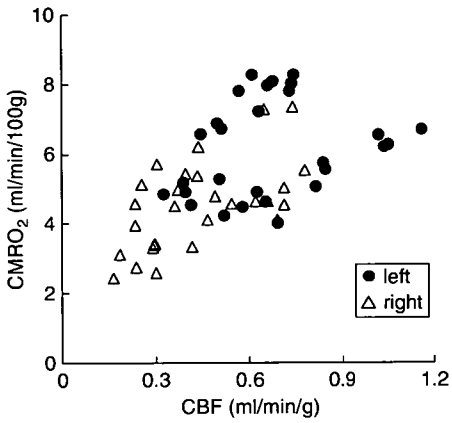

Figure 3 Scatter diagram of CBF (mL/min/g) and $CMRO_2$ (mL/min/100 g) values 1 h after the onset of MCA occlusion.

These two values also exhibit a good correlation, in which the decrease in $CMRO_2$ in the right hemisphere was not so marked.

Studies at 24 h After Onset

The relationships among parameters at 24 h after the occlusion are shown in scatter diagrams (Figures 4 and 5). As shown in Figure 4, in the right hemisphere, the decrease in CBF was more pronounced than at 1 h (Figure 2) and there was no compensatory increase in OEF, resulting in a loss of the good correlation between CBF and OEF. Figure 5 shows the relationship between CBF and $CMRO_2$. The right hemisphere exhibited a marked decrease in $CMRO_2$.

Quantitative Values of Cerebral Blood Flow, Oxygen Extraction Fraction and Cerebral Metabolic Rate for Oxygen

Figure 6 and Table 2 show the averaged hemispheric values of CBF, OEF and $CMRO_2$ at 1 h ($n=7$) and

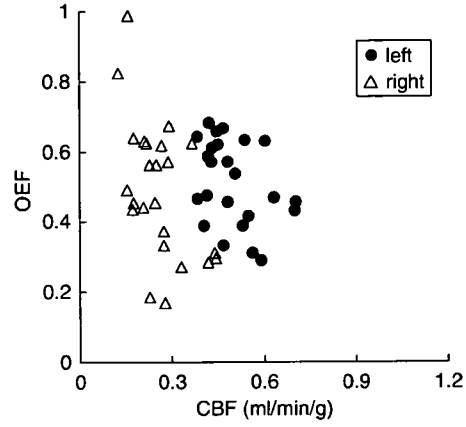

Figure 4 Scatter diagram of CBF (mL/min/g) and OEF values 24 h after the onset of MCA occlusion.

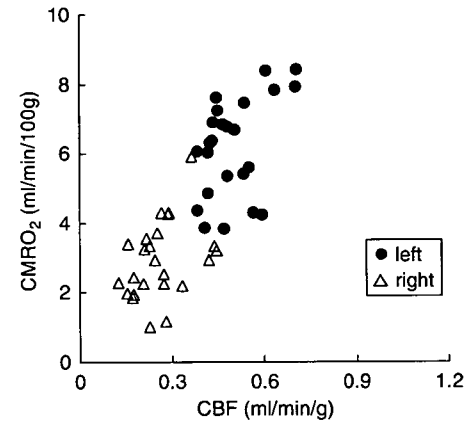

Figure 5 Scatter diagram of CBF (mL/min/g) and $CMRO_2$ (mL/min/100 g) values 24 h after the onset of MCA occlusion.

24 h ($n=6$) after the onset of MCA occlusion. In the right hemisphere at 1 h, the decrease in CBF was not so marked (0.44 ± 0.17 mL/min/g; $P<0.05$ compared with the left side) and a compensatory increase in OEF (0.50 ± 0.19; $P<0.05$ compared with the left side) was observed, inducing a slight decrease in $CMRO_2$ (4.5 ± 1.1 mL/min/100 g; $P<0.05$ compared with the left side). In contrast, at 24 h, there was a marked decrease in CBF (0.26 ± 0.07 mL/min/g, $P<0.05$ compared with both the left side and at 1 h) and no compensatory increase in OEF (0.49 ± 0.19; OEF in the left hemisphere was 0.51 ± 0.12, not significant with each other), resulting in a large decrease in $CMRO_2$ (2.9 ± 0.8 mL/min/100 g; $P<0.05$ compared with both the left side and at 1 h).

Discussion

In our previous report (Magata *et al*, 2003), up to 72 MBq/ml of injectable ^{15}O-O_2 was obtained with

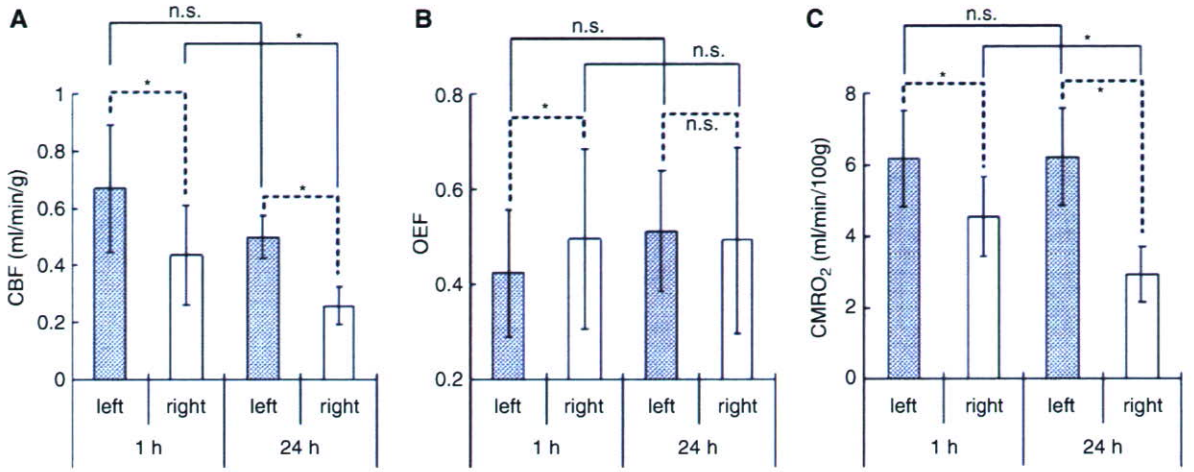

Figure 6 The averaged hemispheric values of (**A**) CBF (mL/min/g), (**B**) OEF and (**C**) $CMRO_2$ (mL/min/100 g) obtained by PET 1 ($n = 7$) and 24 h ($n = 6$) after the onset of MCA occlusion. Significant differences in each parameter (CBF, OEF, $CMRO_2$) between the left and right hemispheres at the same time point and between 1 h and 24 h on the same hemisphere were determined using the Wilcoxon signed-rank test and the Mann–Whitney *U*-test, respectively; $^*P < 0.05$, n.s. not significant.

Table 2 The averaged hemispheric values of CBF (mL/min/g), OEF and $CMRO_2$ (mL/min/100 g) obtained by PET 1 (n = 7) and 24 hours (n = 6) after the onset of MCA occlusion.

	1 h		*24 h*	
	Left	*Right*	*Left*	*Right*
CBF (mL/min/g)	0.67 (0.22)	0.44 (0.17)*	0.50 (0.08)	0.26 (0.07)*,†
OEF	0.42 (0.13)	0.50 (0.19)*	0.51 (0.12)	0.49 (0.19)
$CMRO_2$ (mL/min/100 g)	6.2 (1.3)	4.5 (1.1)*	6.2 (1.4)	2.9 (0.8)*,†

Significant differences in each parameter (CBF, OEF, $CMRO_2$) between the left and right hemispheres at the same time point and between 1 and 24 h on the same hemisphere were determined using the Wilcoxon signed-rank test ($^*P < 0.05$) and the Mann–Whitney *U*-test ($^†P < 0.05$), respectively. Values listed are means (s.d.).

an artificial lung (6 cm length) and about 10 ml of blood. In the present study, the artificial lung was made three times longer to increase the labeling efficiency. First, we used three small artificial lungs connected in series to improve the labeling efficiency. In that system, more blood was needed for summation of the dead volume of each lung, and, the labeling efficiency, radioactivity per unit blood volume, did not increase. Since the total activity in the labeling system is constant if the radioactivity in the supplied gas is constant, highly specific activity of injectable ^{15}O-O_2 can be obtained when a small amount of blood is used. Therefore, the 'long' artificial lung can increase the specific activity of injectable ^{15}O-O_2 owing to the small dead volume. Actually, with this new artificial lung and 18.6 ml of blood, 90 MBq/ml of injectable ^{15}O-O_2 was obtained.

During the experiments, arterial blood gases were analyzed several times (Table 1). At both 1 and 24 h, significant changes were observed in two or three parameters. At 1 h, Hct and Hb decreased after the experiment, indicating slight hemolytic anemia. At 24 h, pO_2, pCO_2 and O_2Sat changed during the PET scans. These values, especially pCO_2, are known to be closely related to the depth of anesthesia and so might reflect a change in the condition of the animal in PET studies. In any case, the changes of these parameters were not so marked and they might not affect the results of experiments.

At 1 h after the onset of MCA occlusion, CBF decreased slightly but significantly in the right hemisphere in comparison with the left side; some ROIs showed normal values and others showed low values (Figure 2). The OEF increased in ROIs with decreased CBF, but not in ROIs with normal CBF (Figure 2). The results indicate that the metabolic compensatory mechanism worked well at 1 h after MCAO. Cerebral metabolic rate for oxygen was also kept in the area of low CBF (Figure 3), and a good correlation between CBF and $CMRO_2$ with a gentle slope was obtained (Figure 3), suggesting that the compensatory mechanism was working well at this time point.

At 24 h after the onset of MCA occlusion, while all ROIs in the right hemisphere showed severely decreased CBF with small variation, OEF showed a

large variation (Figure 4). In the relationship between CBF and $CMRO_2$, all ROIs in the right hemisphere showed severely decreased $CMRO_2$ (Figure 5). These results indicated that the compensatory mechanism at 1 h after MCAO onset had collapsed at 24 h and the progression of ischemic injury was severer than at 1 h.

In Figure 6 and Table 2, quantitative values and standard deviations of CBF, OEF and $CMRO_2$ are summarized. In the right hemisphere, CBF decreased slightly at 1 h and severely at 24 h. Both values were significantly low compared with the opposite sides ($P<0.05$) at both time points and the difference between the 24 h was also significant ($P<0.05$). In the left hemisphere, CBF showed a little decrease but was not significant during 24 h ($P=0.0865$). Since $CMRO_2$ expressed exactly the same values at both time points, the decrease in CBF might not mean a metabolic dysfunction but a vascular disturbance at 24 h. Although blood vessels in the left hemisphere should not be affected directly in our MCAO operation, the progression of the ischemic damage in the right hemisphere included both the spreading of the ischemic core and the disturbance of surrounding blood vessels so that it is considered that the decrease in CBF on the opposite side could have occurred. Furthermore, $CMRO_2$ in the left hemisphere was close to the value obtained previously in normal rats using ^{133}Xe as a CBF tracer and a surgical method for determining OEF (6.3 ± 0.3 mL/min/100 g) (Kozniewska and Szczepanska-Sadowska, 1990). It underlined the preceding discussion that the brain tissue in the left hemisphere was not damaged at all during 24 h and the reason for the little decrease in CBF was vascular disturbance.

In the right hemisphere, $CMRO_2$ decreased severely during 24 h in the same manner as CBF (Figure 6, Table 2). Since these values did not represent $CMRO_2$ in the ischemic core but just values in the entire right hemisphere because of the large size of ROIs, it is difficult to discuss the progression of impairment. However, taken together with the decreases in CBF in both hemispheres during 24 h, the decrease in $CMRO_2$ might not mean an ischemic core-specific progression of tissue disturbance but a spreading of the ischemic damage throughout the hemisphere. In fact, TTC staining revealed no sign of disturbance at 1 h but severe disruption at 24 h in the right hemisphere.

Meanwhile, an obvious change of OEF was also evident during 24 h (Figure 6, Table 2). The increase in OEF in the right hemisphere compared with the left side at 1 h after the onset of MCAO ($P<0.05$) showed that the metabolic compensatory mechanism was working well. However, at 24 h, the OEF was the same in both hemispheres ($P=0.7532$), which indicates that the compensatory mechanism did not function at 24 h after the onset. Therefore, considering that the condition in the left hemisphere at 1 h was actually normal or stage I in the course of the ischemic disorder (Nemoto *et al*, 2004; Powers, 1991), the right hemisphere at 1 h might include partly stage II and stage III (Figures 2 and 3; CBF was normal or decreased, OEF increased and $CMRO_2$ was normal or slightly decreased), the left hemisphere at 24 h might be expressed at stage II (Figures 4 and 5; CBF decreased, OEF increased, $CMRO_2$ was normal) and the right hemisphere at 24 h might include early and severe phases of stage III (Figures 4 and 5; CBF decreased, OEF increased or decreased and $CMRO_2$ strikingly decreased).

Conclusion

In this paper, we estimated the changes in CBF, OEF and $CMRO_2$ after the onset of MCA occlusion in rats by PET using injectable ^{15}O-O_2. In the early phase after occlusion, a decrease in CBF and compensatory increase in OEF were shown, and in contrast, CBF and $CMRO_2$ were severely decreased in the late phase. This is the first report to indicate reliable oxygen metabolism in a MCAO rat model using PET.

References

Baron JC (2001) Perfusion thresholds in human cerebral ischemia: historical perspective and therapeutic implications. *Cerebrovasc Dis* 11(Suppl 1):2–8

Belayev L, Zhao W, Busto R, Ginsberg MD (1997) Transient middle cerebral artery occlusion by intraluminal suture: I. Three-dimensional autoradiographic image-analysis of local cerebral glucose metabolism–blood flow interrelationships during ischemia and early recirculation. *J Cereb Blood Flow Metab* 17:1266–80

Derejko M, Slawek J, Lass P, Nyka WM (2001) Cerebral blood flow changes in Parkinson's disease associated with dementia. *Nucl Med Rev Cent East Eur* 4:123–7

Ginsberg MD (2003) Adventures in the pathophysiology of brain ischemia: penumbra, gene expression, neuroprotection: the 2002 Thomas Willis Lecture. *Stroke* 34:214–23

Heiss WD, Graf R, Lottgen J, Ohta K, Fujita T, Wagner R *et al* (1997) Repeat positron emission tomographic studies in transient middle cerebral artery occlusion in cats: residual perfusion and efficacy of postischemic reperfusion. *J Cereb Blood Flow Metab* 17:388–400

Heiss WD, Graf R, Wienhard K, Lottgen J, Saito R, Fujita T *et al* (1994) Dynamic penumbra demonstrated by sequential multitracer PET after middle cerebral artery occlusion in cats. *J Cereb Blood Flow Metab* 14:892–902

Heiss WD, Kracht LW, Thiel A, Grond M, Pawlik G (2001) Penumbral probability thresholds of cortical flumazenil binding and blood flow predicting tissue outcome in patients with cerebral ischaemia. *Brain* 124:20–9

Kozniewska E, Szczepanska-Sadowska E (1990) V2-like receptors mediate cerebral blood flow increase following vasopressin administration in rats. *J Cardiovasc Pharmacol* 15:579–85

Kuge Y, Minematsu K, Yamaguchi T, Miyake Y (1995) Nylon monofilament for intraluminal middle cerebral artery occlusion in rats. *Stroke* 26:1655–8

Longa EZ, Weinstein PR, Carlson S, Cummins R (1989) Reversible middle cerebral artery occlusion without craniectomy in rats. *Stroke* 20:84–91

Magata Y, Temma T, Iida H, Ogawa M, Mukai T, Iida Y *et al* (2003) Development of injectable O-15 oxygen and estimation of rat OEF. *J Cereb Blood Flow Metab* 23: 671–6

Minematsu K, Li L, Fisher M, Sotak CH, Davis MA, Fiandaca MS (1992) Diffusion-weighted magnetic resonance imaging: rapid and quantitative detection of focal brain ischemia. *Neurology* 42:235–40

Mintun MA, Raichle ME, Martin WR, Herscovitch P (1984) Brain oxygen utilization measured with O-15 radiotracers and positron emission tomography. *J Nucl Med* 25:177–87

Mori S (2002) Responses to donepezil in Alzheimer's disease and Parkinson's disease. *Ann NY Acad Sci* 977: 493–500

Nemoto EM, Yonas H, Kuwabara H, Pindzola RR, Sashin D, Meltzer CC *et al* (2004) Identification of hemodynamic compromise by cerebrovascular reserve and oxygen extraction fraction in occlusive vascular disease. *J Cereb Blood Flow Metab* 24:1081–9

Pappata S, Fiorelli M, Rommel T, Hartmann A, Dettmers C, Yamaguchi T *et al* (1993) PET study of changes in local brain hemodynamics and oxygen metabolism after unilateral middle cerebral artery occlusion in baboons. *J Cereb Blood Flow Metab* 13: 416–24

Powers WJ (1991) Cerebral hemodynamics in ischemic cerebrovascular disease. *Ann Neurol* 29:231–40

Shidahara M, Watabe H, Kim KM, Oka H, Sago M, Hayashi T *et al* (2002) Evaluation of a commercial PET tomograph-based system for the quantitative assessment of rCBF, rOEF and $rCMRO_2$ by using sequential administration of ^{15}O-labeled compounds. *Ann Nucl Med* 16:317–27

Takamatsu H, Tsukada H, Kakiuchi T, Nishiyama S, Noda A, Umemura K (2000) Detection of reperfusion injury using PET in a monkey model of cerebral ischemia. *J Nucl Med* 41:1409–16

Temma T, Magata Y, Mukai T, Kitano H, Konishi J, Saji H (2004) Availability of *N*-isopropyl-p-[(125)I]iodoamphetamine (IMP) as a practical cerebral blood flow (CBF) indicator in rats. *Nucl Med Biol* 31:811–4

Tenjin H, Ueda S, Mizukawa N, Imahori Y, Hino A, Ohmori Y *et al* (1992) Positron emission tomographic measurement of acute hemodynamic changes in primate middle cerebral artery occlusion. *Neurol Med Chir (Tokyo)* 32:805–10

Walovitch RC, Cheesman EH, Maheu LJ, Hall KM (1994) Studies of the retention mechanism of the brain perfusion imaging agent 99mTc-bicisate (99mTc-ECD). *J Cereb Blood Flow Metab* 14(Suppl 1):S4–11

Watanabe M, Okada H, Shimizu K, Omura T, Yoshikawa E, Kosugi T *et al* (1997) A high resolution animal PET scanner using compact PS-PMT detectors. *IEEE Trans Nucl Sci* 44:1277–82

Young AR, Sette G, Touzani O, Rioux P, Derlon JM, MacKenzie ET *et al* (1996) Relationships between high oxygen extraction fraction in the acute stage and final infarction in reversible middle cerebral artery occlusion: an investigation in anesthetized baboons with positron emission tomography. *J Cereb Blood Flow Metab* 16:1176–88

Zhao W, Belayev L, Ginsberg MD (1997) Transient middle cerebral artery occlusion by intraluminal suture: II. Neurological deficits, and pixel-based correlation of histopathology with local blood flow and glucose utilization. *J Cereb Blood Flow Metab* 17:1281–90

Hypertension
Journal of the American Heart Association

Gene Transfer of Hepatocyte Growth Factor Gene Improves Learning and Memory in the Chronic Stage of Cerebral Infarction

Munehisa Shimamura, Naoyuki Sato, Satoshi Waguri, Yasuo Uchiyama, Takuya Hayashi, Hidehiro Iida, Toshikazu Nakamura, Toshio Ogihara, Yasufumi Kaneda and Ryuichi Morishita

Hypertension 2006;47:742-751; originally published online Feb 27, 2006;
DOI: 10.1161/01.HYP.0000208598.57687.3e
Hypertension is published by the American Heart Association. 7272 Greenville Avenue, Dallas, TX 72514

 Print ISSN: 0194-911X. Online ISSN: 1524-4563

Gene Transfer of Hepatocyte Growth Factor Gene Improves Learning and Memory in the Chronic Stage of Cerebral Infarction

Munehisa Shimamura, Naoyuki Sato, Satoshi Waguri, Yasuo Uchiyama, Takuya Hayashi, Hidehiro Iida, Toshikazu Nakamura, Toshio Ogihara, Yasufumi Kaneda, Ryuichi Morishita

Abstract—There is no specific treatment to improve the functional recovery in the chronic stage of ischemic stroke. To provide the new therapeutic options, we examined the effect of overexpression of hepatocyte growth factor (HGF) in the chronic stage of cerebral infarction by transferring the HGF gene into the brain using hemagglutinating virus of Japan envelope vector. Sixty rats were exposed to permanent middle cerebral artery occlusion (day 1). Based on the sensorimotor deficits at day 7, the rats were divided equally into control vector or HGF-treated rats. At day 56, rats transfected with the HGF gene showed a significant recovery of learning and memory in Morris water maze tests (control vector 50±4 s; HGF 33±5 s; $P<0.05$) and passive avoidance task (control vector 132.4±37.5 s; HGF 214.8±26.5 s; $P<0.05$). Although the total volume of cerebral infarction was not related to the outcome, immunohistochemical analysis for Cdc42 and synaptophysin in the peri-infarct region revealed that HGF enhanced the neurite extension and increased synapses. Immunohistochemistry for glial fibriary acidic protein revealed that the formation of glial scar was also prevented by HGF gene treatment. Additionally, the number of the arteries was increased in the HGF group at day 56. These data demonstrated that HGF has a pivotal role for the functional recovery after cerebral infarction through neuritogenesis, improved microcirculation, and the prevention of gliosis. Our results also provide evidence for the feasibility of gene therapy in the chronic stage of cerebral infarction. (***Hypertension.*** **2006;47:742-751.)**

Key Words: cerebral ischemia ■ genes ■ microcirculation ■ rats

Middle cerebral artery occlusion (MCAo) is one of the most common causes of focal stroke in humans[1] and causes severe sensorimotor deficits and cognitive dysfunction. The ischemic changes closely resemble those produced in a MCAo model in rats,[1] which causes infarction mainly in the dorsolateral and lateral portions of the neocortex and the entire caudoputamen.[2] Several growth factors are upregulated immediately after MCAo, such as fibroblast growth factor (FGF),[3] brain-derived neurotrophic factor,[4] glial cell line-derived neurotrophic factor,[5] vascular endothelial growth factor (VEGF),[6] and hepatocyte growth factor (HGF),[7] and thought to protect neurons or promote angiogenesis after MCAo. In fact, the extension of infarction is prevented by administration of growth factors or gene transfer of growth factors before or immediately after MCAo.[8–11] However, the therapeutic time window of such treatment is too short for clinical use,[12] because they focused on preventing the extension of neuronal death in the penumbra in the acute stage.

Recently, HGF and c-Met/HGF have been reported to be upregulated mainly in the peri-infarct region as long as 28 days after permanent MCAo[13] and up to 14 days in FGF[3] or VEGF.[14] HGF is a well-known potent pleiotropic cytokine that exhibits mitogenic, motogenic, and morphogenic activity in a variety of cells.[15–17] Both HGF and the c-Met/HGF receptor of membranes spanning tyrosine kinase are expressed in various regions of the brain.[13] HGF is also involved in the development and maintenance of cortical neurons during differentiation, motogenesis, neuritogenesis, and neuronal survival during the development of the rat cerebral cortex.[18] Interestingly, HGF promotes proliferation and neuronal differentiation of neural stem cells from mouse embryos.[19] In vivo, it has also been demonstrated that HGF promotes angiogenesis in cerebral ischemia in rodents[20–22] without disrupting the blood–brain barrier.[10]

From these viewpoints, we speculated that HGF might play a pivotal role in the functional recovery in the chronic stage of ischemic insult, and its overproduction could improve the cognitive dysfunction. To clarify this speculation, we transferred the human HGF gene into the brain 7 days after MCAo, using the hemagglutinating virus of Japan (HVJ)-

Received October 23, 2005; first decision November 14, 2005; revision accepted January 13, 2006.

From the Division of Clinical Gene Therapy (M.S., N.S., R.M.), Department of Cell Biology and Neuroscience (S.W., Y.U.), Division of Molecular Regenerative Medicine (T.N.), Department of Geriatric Medicine (T.O.), and Division of Gene Therapy Science (Y.K.), Graduate School of Medicine, Osaka University, Osaka; Department of Advanced Clinical Science and Therapeutics (M.S.), Graduate School of Medicine, Tokyo University, Tokyo; and Department of Investigative Radiology (T.H., H.I.), National Cardiovascular Center Research Institute, Osaka, Japan.

Correspondence to Ryuichi Morishita, Division of Clinical Gene Therapy, Graduate School of Medicine, Osaka University, 2-2 Yamadaoka, Suita 565-0871, Japan. E-mail morishit@cgt.med.osaka-u.ac.jp

Hypertension is available at http://www.hypertensionaha.org DOI: 10.1161/01.HYP.0000208598.57687.3e

envelope vector,[10] and examined behavioral tests, MRI, and histological changes. Here, we demonstrated that gene therapy delayed for as long as 7 days improved outcome from ischemic stroke, and HGF is an important growth factor for the recovery of cognitive function in the chronic stage of MCAo through reconstitution of the neuronal network.

Methods

Preparation of HVJ-Envelope Vector

HVJ-envelope vector was prepared as described previously.[24,25] Briefly, virus suspension (15 000 hemagglutinating units) was inactivated by UV irradiation (99 mJ/cm²) and mixed with plasmid DNA (400 μg) and 0.3% Triton-X. After centrifugation, it was washed with 1 mL of balanced salt solution (10 mmol/L Tris-Cl (pH 7.5), 137 mmol/L NaCl, and 5.4 mmol/L KCl) to remove the detergent and unincorporated DNA. After centrifugation, the envelope vector was suspended in 100 mL of PBS. The vector was stored at 4°C until use.

Construction of Plasmids

To produce an HGF expression vector, human HGF cDNA (2.2 kb) was inserted into a simple eukaryotic expression plasmid that uses the cytomegalovirus promoter/enhancer.[26] This promoter/enhancer has been used to express reporter genes in a variety of cell types and can be considered constitutive. The control vector had the same structure as the expression vector plasmid, including the promoter but not containing HGF cDNA. Plasmids were purified with a QIAGEN plasmid isolation kit (Qiagen).

Surgical Procedure

Male Wistar rats (270 to 300 g; Charles River Japan, Atsugi, Japan) were used in this study. To generate a permanent MCAo model, the right middle cerebral artery (MCA) was occluded by placement of poly-L-lysine-coated 4-0 nylon around the origin of the MCA, as described previously.[7] In vivo gene transfer was performed by intracisternal injection as described previously.[10] Briefly, rats were anesthetized with ketamine (Sankyo) and xylazine (Bayer Ltd). HVJ-envelope vector (100 μL) containing the human HGF gene was infused at 50 μL/min after removing 100 μL of cerebrospinal fluid (CSF). The protocol was approved by the Committee on the Ethics of Animal Experiments in the Osaka University. To examine transfection of the HGF gene in the CSF, CSF (100 μL) was collected 4, 7, 14, and 21 days after gene transfer. The concentration of HGF was determined by enzyme immunoassay using anti-human HGF antibody (Institute of Immunology, Tokyo, Japan) as described previously.[10]

Protocol for Treatment and Behavioral Tests

Ten rats were only anesthetized (sham operation), and 60 rats were subjected to MCAo (day 1). Based on the neuromuscular function and body weight evaluated on day 7, the rats were divided equally into control vector-treated (n = 23) and HGF-treated (n = 23) groups. Rats showing no palsy on day 7 or that died before day 7 were excluded from the present study (n = 14). On day 55, neuromuscular function and locomotor activity were evaluated in the surviving rats (n = 20 for control vector-treated and n = 22 for HGF-treated rats). Then, cognitive function was examined by Morris water maze (MWM) and passive avoidance task from day 56 to 90. On day 96, MRI was performed to evaluate the volume of infarction.

Sensorimotor Deficit and Locomotor Activity

Although there are various batteries for testing sensorimotor deficit, we used a simple protocol[27] to evaluate sensorimotor deficit, which used the following categories (maximum score is 4). For forelimb flexion, rats were held by the tail on a flat surface. Paralysis of the forelimbs was evaluated by the degree of left forelimb flexion. For torso twisting, rats were held by the tail on a flat surface. The degree of body rotation was checked. For lateral push, rats were pushed either left or right. Rats with right MCA occlusion showed weak or no resistance against a left push. For hind limb placement, one hind limb was removed from the surface. Spontaneous locomotor activity was also measured via the open field test for 30 minutes using an automated activity box (Muromachi Kikai).

MWM Task

A cylindrical tank 1.5 m in diameter was filled with water (25°C), and a transparent platform 15 cm in diameter was placed at a fixed position in the center of 1 of the 4 quadrants (O'Hara & Co. Ltd.). In the hidden platform test, the platform was set below the water level, and it was not seen by the rats. The platform was fixed at 1 quadrant, and the starting point was changed in each trial. A previous study showed a difference in the latency of reaching the platform until day 6 of the session between rats exposed to MCAo 12 to 14 weeks before and control rats, if the tests were performed twice a day.[28] Based on the results, we carried out the tests twice a day for 6 days. If the rat could not reach the platform, the latency was set at 60 s. In the visible platform test, a flag was placed on the platform, which could be seen by the rats. The tests were carried out twice a day for 6 days. In this trial, the platform and the starting point were changed in each trial. Throughout the tests, the path of swimming was captured by a charge-coupled device video camera and analyzed by National Institute of Health image.

Passive Avoidance Task

A step-through type of passive avoidance task was used in the present study. The apparatus (Medical Agent) consisted of an illuminated chamber and a dark one. To habituate the rats, they were placed in the illuminated chamber, and the door was opened so that they could enter the dark one. Rats have a habit of entering the dark chamber, because they prefer darkness. In an acquisition trial, the rats were placed in the illuminated chamber and exposed to a 0.6-mA foot shock when they entered the dark chamber. Each trial was continued until the rat learned not to enter the dark chamber for 300 seconds. In retention trials, they were placed in the illuminated room 3 days after the acquisition trial. We evaluated the latency (maximum 300 s) of them staying in the illuminated room.

Immunohistochemical Study

For histopathologic analysis, other rats (control vector-treated [n = 4] or HGF-treated [n = 4] rats in each experiment) were treated the same as described above and euthanized on day 11, 14, or 56, followed by transcardial perfusion fixation with normal saline followed by 4% paraformaldehyde. The brain was removed, postfixed, cryoprotected, and cut on a cryostat at 12 μm. After blocking, sections were incubated in 3% normal goat serum and anti-MAP2 (1:1000; mouse monoclonal; Sigma-Aldrich, St Louis, MO), GFAP (1:1000; mouse monoclonal; Sigma-Aldrich), and Cde42 (1:100; mouse monoclonal; Santa Cruz Biotechnology, Santa Cruz, CA) followed by anti-mouse goat fluorescent antibody (1:1000 for MAP2 and GFAP, 1:250 for Cde42, Alexa Flour 546, Molecular Probes). For immunostaining of human HGF or synaptophysin, sections were treated with 2% H_2O_2 to block endogenous peroxidase and then incubated with an antibody against human HGF-β (H714; 1:250; rabbit polyclonal; Immuno-Biological Laboratories, Gunma, Japan) or synaptophysin (1:500; mouse monoclonal; Chemicon, Temecula, CA) at 4°C O/N. They were incubated with streptavidin-horseradish peroxidase (Vectastain Elite ABC, Vector Laboratories, Burlingame, CA), and the biotin-streptavidin-peroxidase complex was detected with diaminobenzidine (human HGF) or tetramethylbenzidine (synaptophysin) peroxidase substrate solution (Vector Laboratories). Negative control sections from each animal received identical preparations for immunohistochemical staining, except that primary antibodies were omitted.

Quantitative Histological Analysis

To quantify the immunoreactivity for GFAP and synaptophysin, the acquired image was imported into Adobe Photoshop (version 7.0, Adobe System). The color image was converted into a grayscale image. This was imported into Mac SCOPE (version 2.5, Mitani Corporation). The region of interest was set at the peri-infarct region

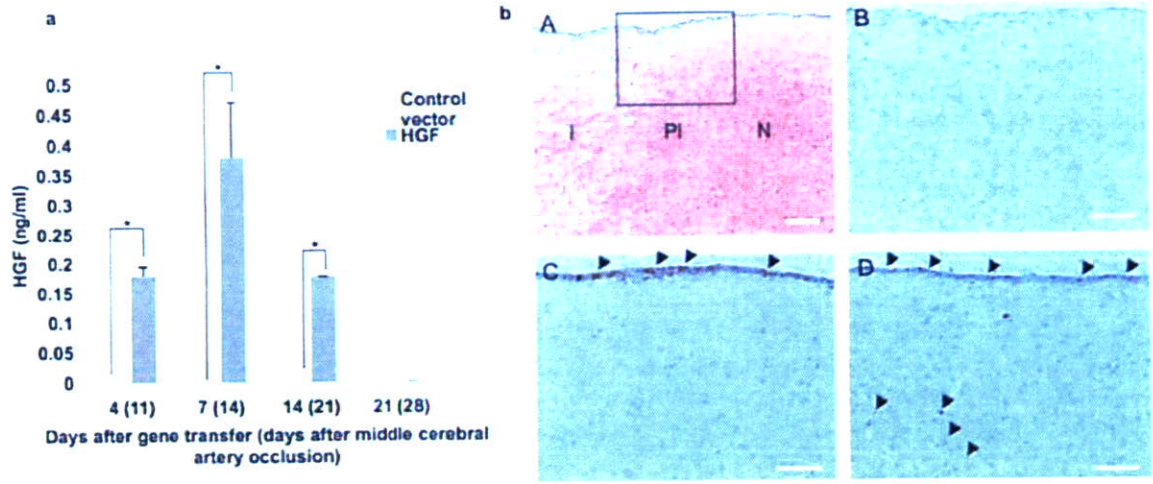

Figure 1. (a) Concentrations of human HGF in cerebrospinal fluid at 4, 7, 14, and 21 days after gene transfer (11, 14, 21, and 28 days after middle cerebral artery occlusion). Control vector indicates rats transfected with control vector (n=4); HGF, rats transfected with HGF vector (n=4). *$P<0.01$ vs Control. (b, part A) HE staining at 4 days after gene transfer (11 days after middle cerebral artery occlusion). I, infarct region; PI, peri-infarct region; N, normal region. Bar=100 μm. (B through D) Representative images of immunohistochemical staining for human HGF. (B) Peri-infarct region in rats transfected with control vector (rectangle area in A). Bar=50 μm. (C) Contralateral intact region in rats transfected with HGF vector. Bar=50 μm. (D) Peri-infarct region in rats transfected with HGF vector. Arrowhead showed immunopositive cells for human HGF. Bar=50 μm.

in the cerebral neocortex. The peri-infarct region is defined as the area surrounding the lesion, which morphologically differs from the surrounding normal tissue (Figure 1b, part A).[29,30] The number of pixels for which the signal was >25 was counted. Immunoreactivity was calculated by the equation: % Area=(Number of high signal pixels)/(Total number of pixels). To quantify the cerebral edema, we calculated the percentage of measured infarct area in the corrected infarct area at 0.7 mm from bregma. The corrected infarct area was calculated as [LT-(RT-RI)], where LT is the area of the left hemisphere, RT is the area of the right hemisphere, and RI is the infarct area.[30] The infarct region is edematous when the percentage is >100%. The infarct brain is atrophic if the percentage is <100%.

Alkaline Phosphatase Staining

For alkaline phosphatase (ALP) staining, sections were washed in Tris-HCl and incubated for 30 minutes in substrate solution (a mixture of naphtol AS-BI phosphate [α-Aldrich] and fast red violet LB salt [α-Aldrich]). Five consecutive sections in each rat were observed, and acquired images were imported into Adobe Photoshop. The color image was converted into a grayscale image. Then, the ROI was set as the region in the peri-infarct region. The area or length of vessels was analyzed with an Angiogenesis Image Analyzer (version 1.0, Kurabo).

Statistical Analysis

All of the values are expressed as mean±SEM. ANOVA was used to determine the significance of differences in multiple comparisons. $P<0.05$ was considered significant.

Results

Transfer of HGF Gene Improves Learning and Memory After Cerebral Infarction

To test for successful gene transfer via the subarachnoid space, the concentration of human HGF in CSF was measured by ELISA at 4, 7, 14, and 21 days after gene transfer. As expected, human HGF could be detected in the CSF of rats transfected with human HGF vector 4 at 7 days after gene transfer, whereas human HGF protein could not be detected in control rats (Figure 1a). Human HGF protein was detected in the pia mater in the

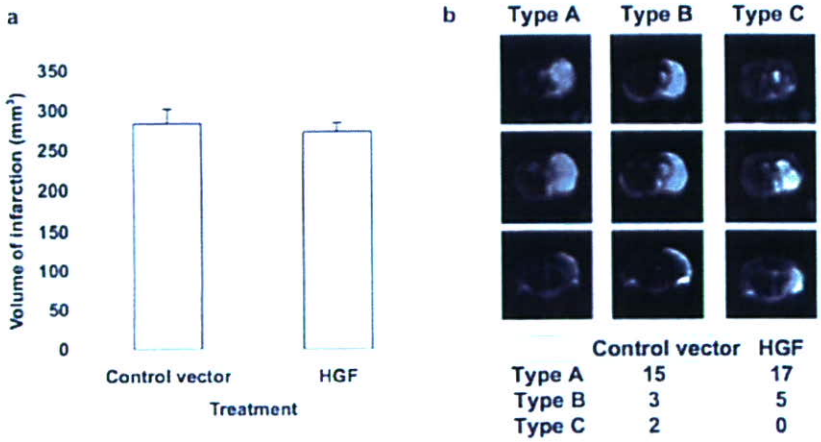

Figure 2. Magnetic resonance images of brain. (a) Volume of infarction in all rats calculated in T2-weighted images. Control vector indicates rats transfected with control vector (n=20); HGF, rats transfected with HGF vector (n=22). (b) Typical T2-weighted image of coronal section of rat brain. The images were divided into 3 groups: types A, B, and C (described in text). Most rats showed type A, and fewer showed type B or type C.

normal region (Figure 1b, part C), as well as in the pia mater and parenchyma in the infarct and peri-infarct region 4 days after gene transfer using immunohistochemistry (Figure 1b, part D). Although HE staining at 4 days after gene transfer showed that the infarct brain is atrophic in this timing, as reported previously,[31] there was no significant difference between rats transfected with the human HGF gene and control vector (control vector 87.1±8.1%, HGF 81.0±4.3%; P value not significant).

To confirm the severity of cerebral infarction, all of the rats were examined by T2-weighted MRI on day 96. Although the total volume of infarction calculated in T2-weighted images was not different between rats transfected with the human HGF gene and control vector (Figure 2a), the pattern of cerebral infarction was divided into 3 groups: (1) type A, high-intensity area seen in the dorsolateral and lateral portions of neocortex and the entire caudoputamen; (2) type B, high-intensity area seen in the dorsolateral and lateral portions of neocortex and in part of the caudoputamen; and (3) type C, high-intensity area seen in part of the lateral neocortex and caudoputamen (Figure 2b). In type C, most part of lateral neocortex was intact.

In the hidden platform test of MWM, which examined spatial learning and memory, the latency in rats transfected with control vector was markedly longer as compared with sham-operated rats, and the latency in rats transfected with HGF vector was significantly shorter than that of rats transfected with control vector (Figure 3a). There were no differences both in swimming speed and visible platform test, which excluded the possible influences of visual loss, sensorimotor deficit, and motivation on the results,[32] between rats transfected with control and HGF vector (data not shown). Thus, spatial learning and memory partly, but significantly, recovered in rats transfected with HGF vector. In the passive avoidance task, which was used to measure associated learning and memory,[32] the retention of memory was longer in rats transfected with the HGF vector (Figure 3b), which demonstrated a trend toward significance ($P=0.053$). Sensorimotor deficit and locomotor activity were also tested, because they have some influence on tests of cognitive function.[33] Sensorimotor deficit had spontaneously recovered to some extent by day 55 in both groups, and there was no difference between the

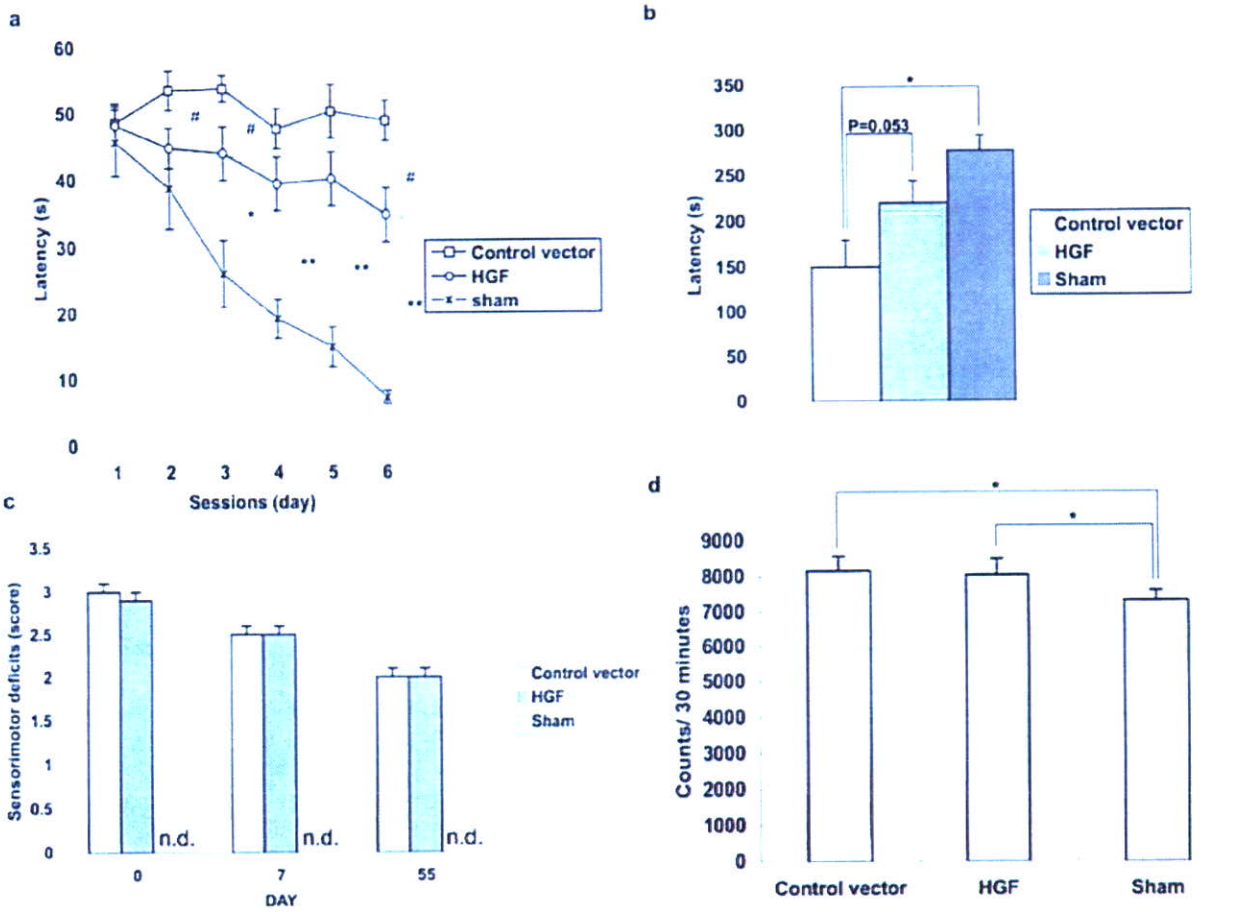

Figure 3. Learning and memory in the chronic stage of cerebral infarction. (a) Hidden platform test in MWM test in all rats. Although rats subjected to middle cerebral artery occlusion hardly reached the hidden platform as compared with sham-operated rats, rats transfected HGF vector could reach faster than that of control vector. (b) Retention trial in passive avoidance task in all rats. The latency of rats staying in the illuminated chamber was calculated. (c) Sensorimotor deficit and (d) spontaneous locomotor activity in all rats. There is no sensorimotor deficit in sham-operation rats in "c" (shown as "n.d."). Control vector indicates rats transfected with control vector (n=20); HGF, rats transfected with HGF vector (n=22); Sham, sham-operated rats (n=10). *$P<0.05$, **$P<0.01$ vs Sham, #$P<0.05$ vs Control.

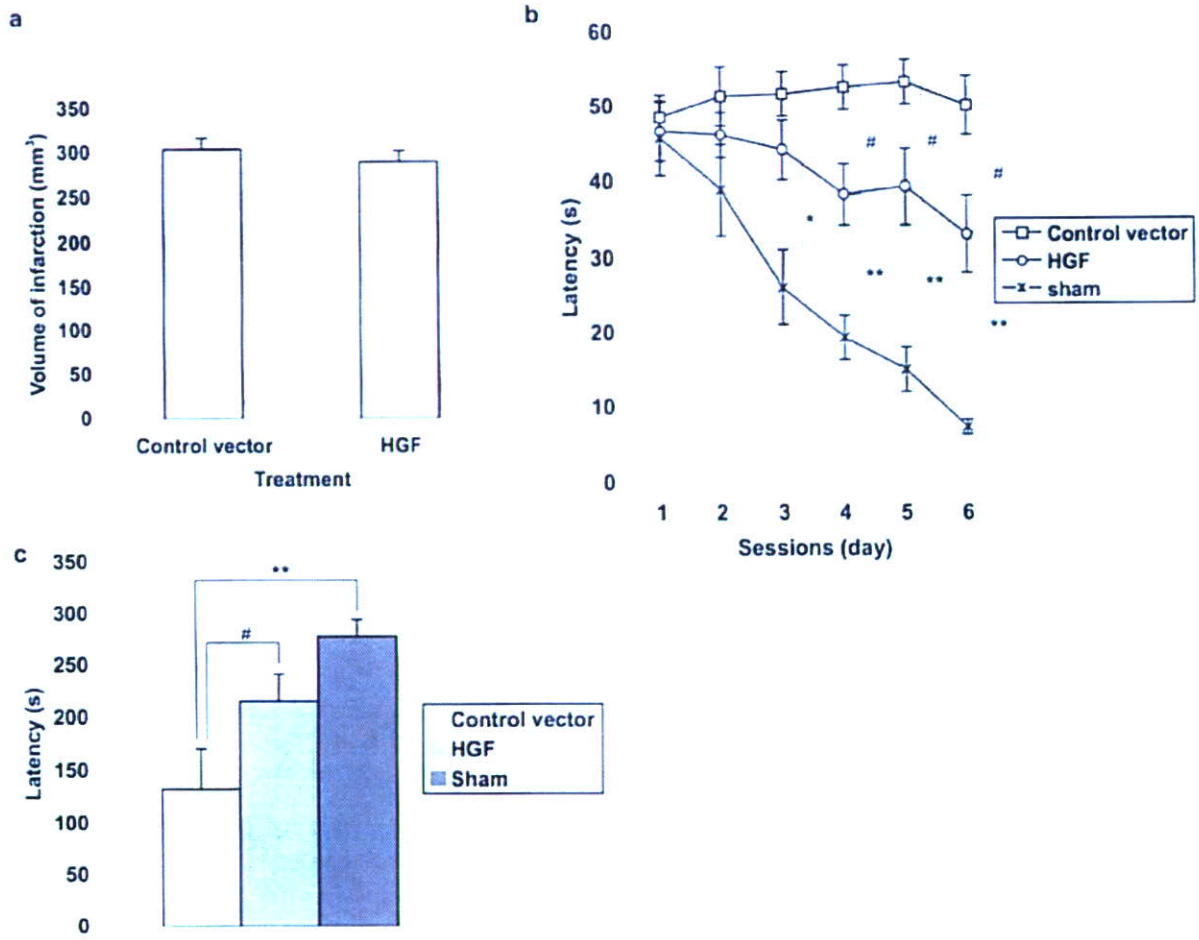

Figure 4. (a) Volume of infarction in type A rats. (b) Hidden platform test in MWM test in type A rats. (c) Retention trial in passive avoidance task in type A rats. Control vector indicates rats transfected with control vector (n=15); HGF, rats transfected with HGF vector (n=17); Sham, sham-operated rats (n=10). $^{*}P<0.05$, $^{**}P<0.01$ vs Sham, $^{\#}P<0.05$ vs Control.

2 groups (Figure 3e). Locomotor activity of rats subjected to MCAo was increased as compared with sham-operated rats, as described before,[33] but there was no difference in rats transfected with control and HGF vector (Figure 3d).

To exclude the influence of the pattern of cerebral infarction on the cognitive function, we additionally focused on type A rats. The volume of cerebral infarction in type A rats was not different between rats transfected with human HGF gene and control vector (Figure 4a). Even type A rats transfected with HGF vector showed the improvement in the learning and memory in MWM test (Figure 4b). Also, rats transfected HGF vector showed the significantly longer retention of memory in the passive avoidance task (Figure 4c). Type A rats showed no significant difference in sensorimotor deficit and locomotor activity (data not shown).

These data supported the results that in the MWM and passive avoidance task were not influenced by the sensorimotor and locomotor activity and the volume and pattern of cerebral infarction. Overall, these data suggest that rats transfected with HGF vector maintain their memory longer as compared with those transfected with control vector.

HGF Enhances Neuritogenesis and Synaptogenesis

To examine whether HGF induced neuritogenesis and/or synaptogenesis, we focused on Cdc42, which belongs to the Rho family of GTPases and has positive effects on neuronal process extension,[34] and synaptophysin, which is used as presynaptic markers and synaptogenesis.[35,36] According to previous reports that the neuronal process extension occurred until 14 days after focal cerebral ischemia[36] and synaptogenesis in the chronic stage of the insult,[36] we measured the immunopositive cells against Cdc42 at day 14 and synaptophysin at day 56. Although the number of Cdc42-positive neurons was the same in the contralateral neocortex in both groups, the peri-infarct region in the neocortex of rats transfected with the HGF vector showed a significant increase in the number of Cdc42-immunoreactive cells (Figure 5a and 5b). Also, the immunoreactivity of synaptophysin was significantly increased at day 56 in rats transfected with the HGF gene, especially in the peri-infarct region (Figure 5c and 5d).

HGF Prevents Glial Scar Formation

Then, we investigated whether HGF had influences on astrocytes, because the neuron–glia interaction is also impor-

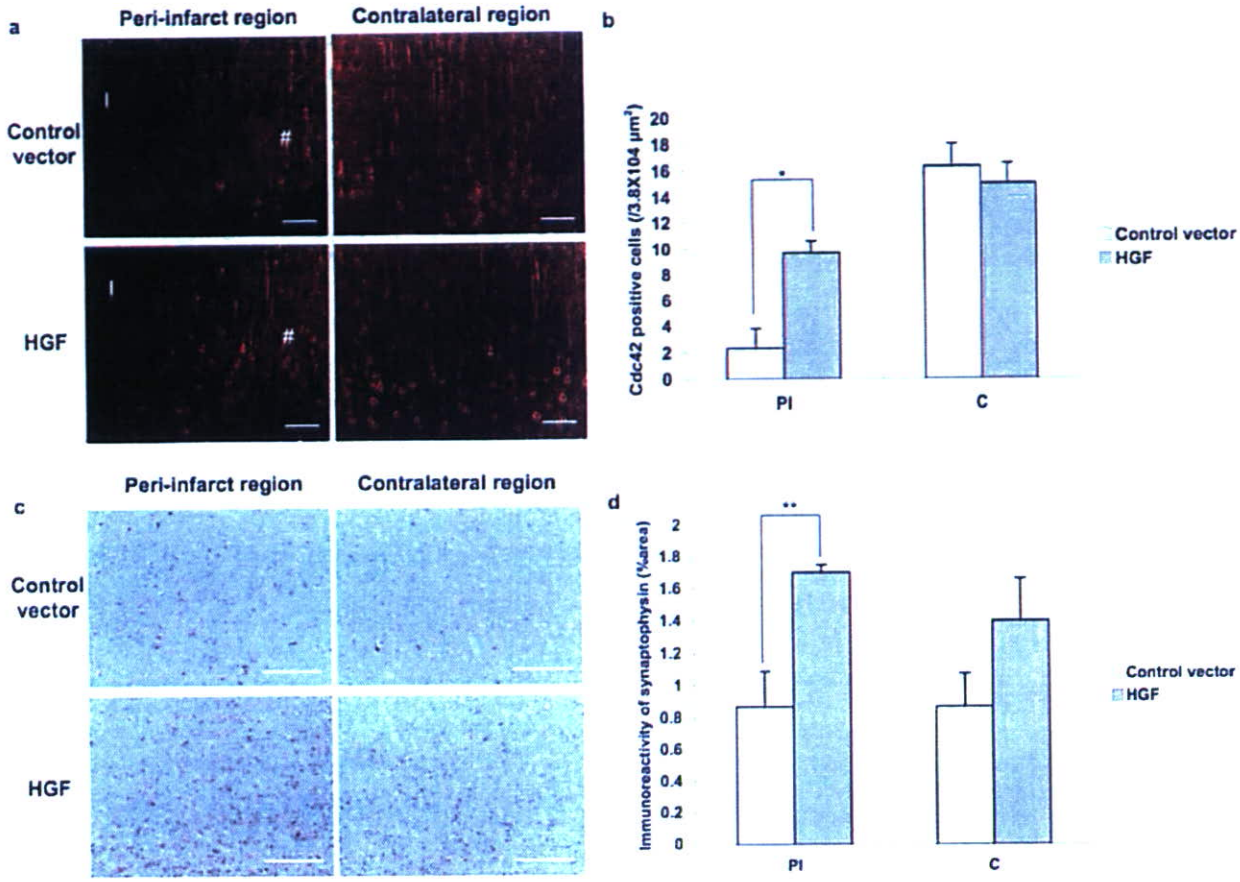

Figure 5. (a) Representative images of immunohistochemical staining for Cdc42 on day 14 in rats transfected with control and HGF vector. The number of cells immunoreactive for Cdc42 was significantly increased in the pyramidal neurons in the peri-infarct region (#) of rats transfected with HGF vector. I, infarct region. (b) Quantitative analysis for Cdc42-immunoreactive cells in peri-infarct region (#). (c) Typical images of immunohistochemical staining for synaptophysin on day 56 (●). (d) Quantitative analysis for the immunoreactivity of synaptophysin. In the peri-infarct region, the immunoreactivity was significantly increased in rats treated with HGF gene. Control vector indicates rats transfected with control vector (n=4); HGF, rats transfected with HGF vector (n=4). *$P<0.05$, **$P<0.01$ vs Control. Bar=100 μm. PI, peri-infarct region in neocortex; C, contralateral region in neocortex.

tant for neuroprotection or neuritogenesis.[17] The immunoreactivity of GFAP was increased on days 14 and 56 in the peri-infarct region in both groups, and the immunoreactivity on day 14 was significantly higher in rats transfected with HGF vector (Figure 6). In contrast, the fewer immunopositive cells against GFAP could be detected in rats transfected with the HGF vector on day 56 as compared with the control vector (Figure 6).

Because some viral vectors, such as adenoviral vector, cause diffuse encephaloventriculitis and substantial leukoencephalopathy,[18] we also performed hematoxylin/eosin staining to examine the inflammation. As expected, there was no inflammatory lymphocyte infiltration in HGF and control vector–transfected rats compared with sham-operated rats (data not shown).

HGF Increases Microvessels in the Peri-Infarct Region

Finally, the arteries in the peri-infarct and contralateral region were also examined using ALP staining on days 14 and 56. In the peri-infarct region, on day 56, arteries were significantly increased in rats transfected with HGF vector as compared with control vector (Figure 7a). Consistently, quantitative analysis showed an increase in the area and length of arteries on day 56 in the peri-infarct region in rats transfected with HGF vector (Figure 7b and 7c). Of importance, in the contralateral region, there was no difference between the groups on days 14 and 56 (Figure 7b and 7c).

Discussion

Disruption of blood flow to the brain initiates a cascade of events that produces neuronal death and leads to neurological dysfunction. From this viewpoint, we and others have reported that pretreatment with neurotrophic factors, such as FGF and HGF, has beneficial effects to prevent brain injury. However, considering their clinical application, pretreatment with neurotrophic factors might not be feasible. Unfortunately, few reports have revealed beneficial effects of treatment after infarction. To develop new therapeutic strategies to treat brain infarction, in this study, we examined the effects of overexpression of HGF after infarction, because HGF has unique actions in the central nervous system, as (1) a survival

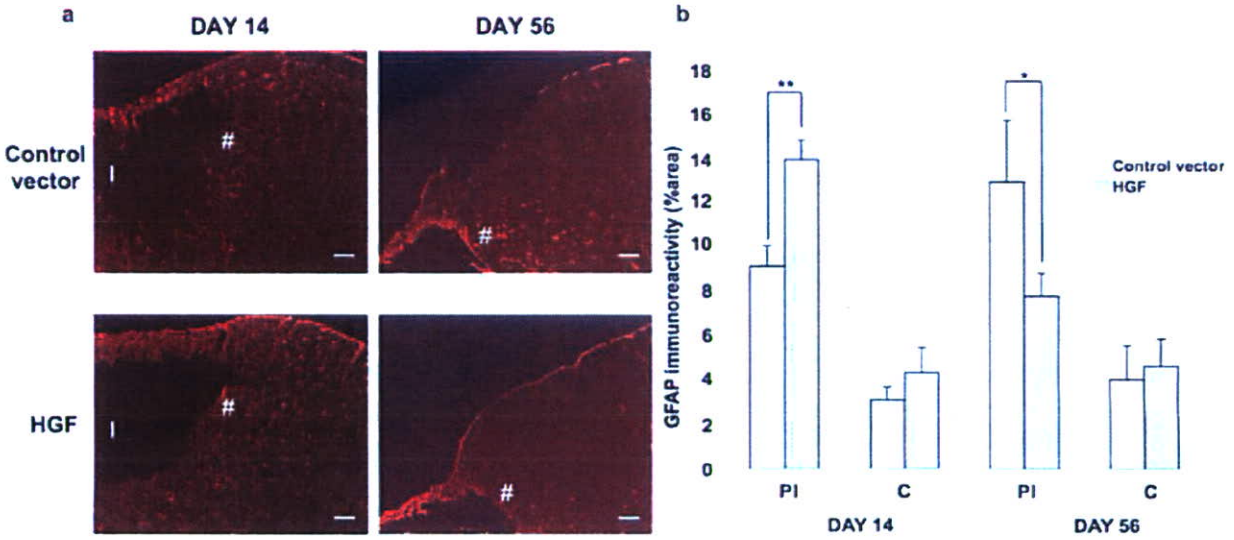

Figure 6. (a) Representative images of immunohistochemical staining for GFAP in ipsilateral neocortex on day 14 and 56 in rats transfected with control and HGF vector. Positive staining for GFAP was increased on day 14 and decreased on day 56 in the peri-infarct region (#) in rats transfected with HGF vector. I indicates infarct region (n=4 in each group; bar=100 μm.) (b) Quantitative analysis of immunoreactivity for GFAP in neocortex. PI, peri-infarct region in neocortex; C, contralateral region in neocortex. Control vector, rats transfected with control vector (n=4); HGF, rats transfected with HGF vector (n=4). *$P<0.05$, **$P<0.01$ vs Control.

factor for embryonic motor neurons; (2) a stimulatory factor for the differentiation, survival, and axonal outgrowth of sensory and sympathetic neurons; (3) a neurotrophic factor;[39] and (4) a potent angiogenic growth factor.[40,41] The present study demonstrated that overexpression of HGF resulted in significant improvement of the results in MWM and the passive avoidance task on day 56, without any difference in infarct size and pattern. This study demonstrated that treatment with HGF postinfarction improved learning and memory.

Interestingly, the overexpression of HGF did not act on the disability of sensorimotor function and locomotor activity. The discrepancy of the recovery between the sensorimotor and cognitive functions has also been reported recently.[30] The authors reported that the functional recovery was observed not in the cognitive function but in the sensorimotor deficits when MHP36 stem cells were grafted into the cerebral parenchyma, whereas only spatial learning was improved in rats with intraventricular grafts.[30] Although the reason why the discrepancy was caused was unclear in the present study, we speculate that the functional recovery might be dependent on the kind of growth factor or the route of administration because of the different mechanisms in recovery from sensorimotor and cognitive deficits. Because the improvement of the sensorimotor deficits is also important, additional study is necessary to achieve the improvement of sensorimotor deficits.

The region where the significant histological difference was observed was the peri-infarct region, which was the border region between the frontal and parietal cortex. Because the neocortex was also an important site for learning and memory,[31] we speculate that the functional recovery enhanced by HGF is dependent on that region in the present study. In fact, both the immunohistochemical analysis for Cdc42, synaptophysin, and GFAP and the ALP staining revealed significant differences in that region. Cdc42 belongs to the Ras superfamily of small GTPases and is expressed in hippocampus, cerebellum, thalamus, and neocortex in the rats.[34,42] In general, Rac and Cdc42 have positive effects on process extension, whereas Rho has a positive effect on process retraction. HGF activated Cdc42, concomitant with the formation of filopodia and lammelipodia, in epithelial cells,[43] although it was not still demonstrated in neurons. Considering that the immunoreactivity for Cdc42 in pyramidal neurons, which possess a high density of cholinergic terminals,[44] was enhanced at day 14, the reconstitution of the neural network through neurite extension, so-called "neuritogenesis," might be in progress at the early stage of HGF gene treatment. Also, the immunoreactivity of the presynaptic marker synaptophysin was increased at day 56 in rats treated with the HGF gene, which implies that the neuritogenesis resulted in the formation of new synapses.[35,36] These results suggested that HGF enhanced neuritogenesis and synaptogenesis, which might contribute to the recovery of cognitive dysfunction.

The association of neurogenesis is also the center of interest, because HGF is involved in the development and maintenance of cortical neurons during differentiation and motogenesis in the neocortex.[38] In general, adult neurogenesis in the neocortex is still controversial.[44,45] It is also unclear whether adult neurogenesis occurs in the neocortex in rats after focal cerebral ischemia, because Jiang et al[46] showed the existence of neurogenesis, but Zhang et al[47] failed to detect neuronal nuclei and 5-bromodeoxyuridine double-labeling cells in the neocortex. In the present study, the fact that the volume of infarction was not decreased by transfection of the HGF gene and the density of matured neurons assessed by immunohistochemistry for MAP2 was not different (data not shown) implied that neurogenesis was not related to the functional recovery.

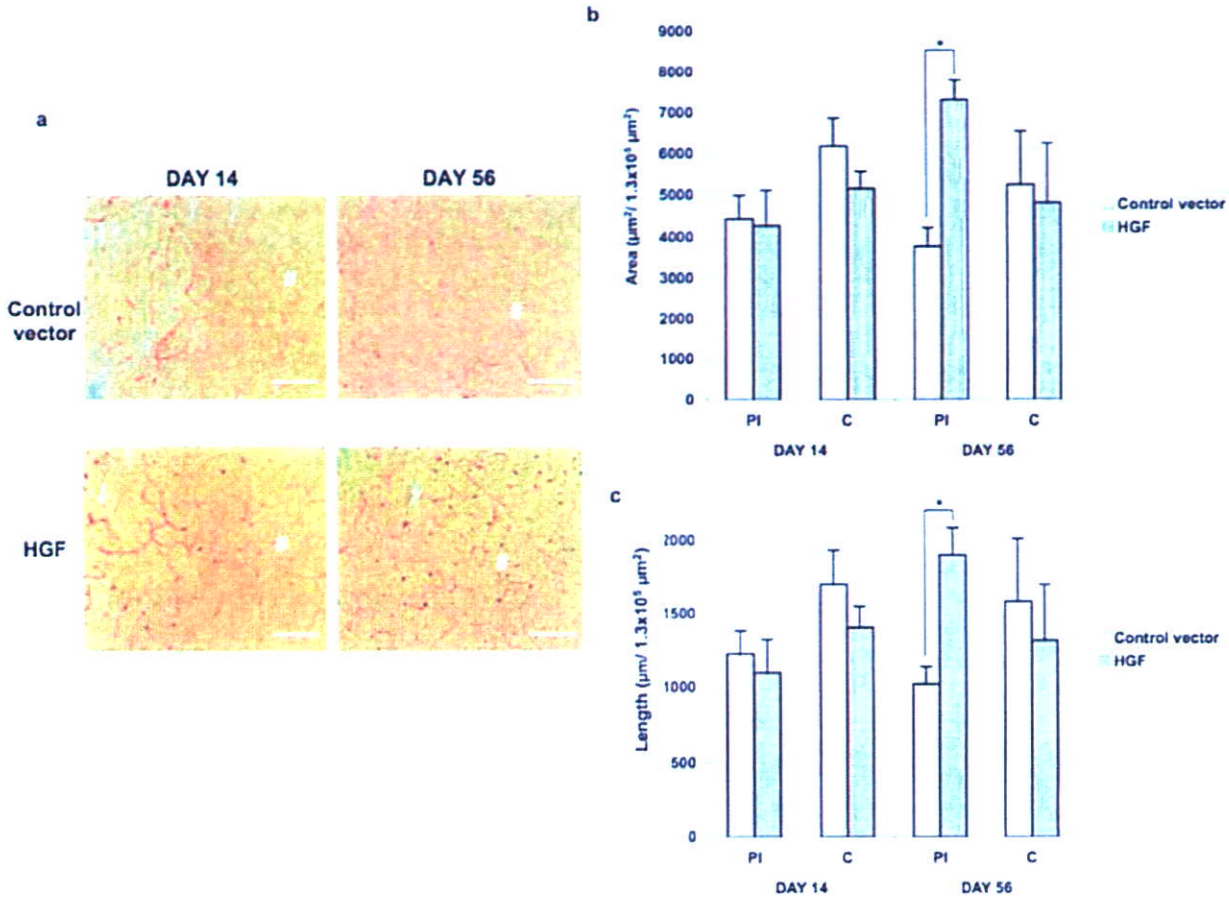

Figure 7. (a) Typical images of ALP staining in ipsilateral neocortex on day 14 in rats transfected with control and HGF vector. Coronal sections of ipsilateral neocortex stained for ALP. The structure of arteries in the peri-infarct region (#) was not different on day 14. However, the arteries in rats transfected with HGF gene showed a more complex pattern on day 56. Bar = 100 μm; I indicates infarct region. (b and c) Quantitative analysis of area (b) and length (c) of blood vessels. PI, peri-infarct region; C, contralateral region; Control vector, rats transfected with control vector (n = 4); HGF, rats transfected with HGF vector (n = 4). *$P<0.05$ vs Control.

Another possible mechanism is that exogenously added HGF would transiently activate astrocytes and induce the production of other neurotrophic factors, resulting in the promotion of neuritogenesis. In fact, immunoreactivity for GFAP was increased on day 14 but decreased on day 56 to the contrary. Similar results were also observed in the recent report showing the effectiveness of forced arm use and brain-derived neurotrophic factor in MCAo.[35] A recent study showed that the activated astrocytes possess qualities that will promote neuronal survival and regeneration, and they do not, by themselves, produce inhibitory extracellular matrix, whereas reactivated astrocytes stimulated by cytokines, including interleukin 1b, interferon γ, tumor necrosis factor α, and transforming growth factors, contribute to the glial scar formation, which inhibit neuronal survival or regeneration.[37] It was also demonstrated that exogenous HGF regulated c-Met expression in cultured astrocytes and might induce other neurotrophic factors from activated astrocytes.[38] Thus, it is likely that the effect of HGF was direct action and/or indirect action via neuron–glia interactions on neuritogenesis.

This study also revealed an increase in microvessels only in the peri-infarct region but not in normal regions. Although the relationship between the improved microcirculation and behavior is still unclear, a recent report demonstrated that restoration of perfusion by collateral growth and new capillaries in the ischemic border zone around a cortical infarct supported long-term functional recovery in rats.[39] Additionally, others reported that some patients who received tissue plasminogen activator therapy with no immediate clinical improvement in spite of early recanalization showed delayed clinical improvement.[30] From the viewpoints, it is likely that the improvement of microcirculation is an important factor for the functional recovery. Although additional study is necessary, the improvement of microcirculation by HGF might be an alternative mechanism to improve learning and memory.

The influence of HGF on cerebral edema is another important issue. In general, the peak of cerebral edema is 3 days, and a significant decrease is 7 days after permanent MCAo in rats.[31] Afterward, the infarct brain becomes atrophic.[3] In the present study, the infarct region was atrophic in rats transfected with the HGF gene, as well as the control vector, and there was no significant difference in the volume. Thus, HGF gene transfer did not exacerbate the cerebral edema. Considering that VEGF

exacerbated cerebral edema.[53] HGF might be safer than VEGF. Additional study is necessary to compare the effectiveness of HGF to other growth factors.

The amount of HGF produced by this method (0.1 to 0.4 ng/mL) is relatively low because of the limited transfected cells in the surface brain and ischemic region, as compared with that of previous reports showing the effectiveness of recombinant human HGF protein for the cerebral ischemia.[14,23] Nevertheless, this low concentration might be enough to have the beneficial effects, because HGF elicited surviving neurotrophic effect at 0.5 to 1 ng/mL in primary cultured hippocampal neurons[17] and enhanced neurite extension at 0.1 to 100 nM (0.1 to 100 ng/mL) in neocortical explant.[52] Indeed, several previous articles demonstrated that the similar amount of HGF produced by gene transfer showed the neurotrophic and/or angiogenic property in several experimental rodent models.[21,22,25,54] Because the higher concentration of HGF is more effective for survival and neurite extension in in vitro study,[17,52] several improvements, such as modification of the HVJ-envelope vector and HGF plasmid, are required to achieve better outcome.

Perspectives

Overall, the present study is the first to demonstrate that HGF gene therapy delayed for as long as 7 days improved the outcome from ischemic stroke through the reconstitution of the neuronal network and improvement in the microcirculation. In clinical use, the present study might be attractive to support the application of HGF for the treatment of the patients in the chronic stage of brain infarction. Although most of the previous reports demonstrated the effectiveness of growth factors before the insult or within several hours of the onset by the inhibition of apoptosis and extension of the ischemic lesion,[9,10,12,21,22] it is difficult to administer them in time in most patients. Additionally, some patients improve their cognitive dysfunction spontaneously within several days after cerebral infarction. Also, the intracisternal injection is too difficult in the acute stage of cerebral infarction, because it is possible that the brain edema is worsened by intracisternal injection itself. In contrast, the present study is more closed to the real clinical situation for the treatment of the patients with chronic brain stroke. Although additional study is necessary to determine whether other growth factors are effective or not in the chronic stage, gene therapy using HGF may provide new therapeutic options for treatment after cerebral ischemia.

Acknowledgments

This work was partially supported by a grant-in-aid from the Organization for Pharmaceutical Safety and Research, a grant-in-aid from the Ministry of Public Health and Welfare, a grant-in-aid from Japan Promotion of Science, and a grant-in-aid from the Ministry of Education, Culture, Sports, Science and Technology of the Japanese Government.

References

1. Hunter AJ, MacKay KB, Rogers DC. To what extent have functional studies of ischaemia in animals been useful in the assessment of potential neuroprotective agents? *Trends Pharmacol Sci*. 1998;19:59–66.
2. Belayev L, Alonso OF, Busto R, Zhao W, Ginsberg MD. Middle cerebral artery occlusion in the rat by intraluminal suture: Neurological and pathological evaluation of an improved model. *Stroke*. 1996;27:1616–1623.
3. Lin TN, Te J, Lee M, Sun GY, Hsu CY. Induction of basic fibroblast growth factor (bFGF) expression following focal cerebral ischemia. *Brain Res Mol Brain Res*. 1997;49:255–265.
4. Arai S, Kitagawa H, Akahane A, Owada Y, Kamii H, Kawase M, Yoshimoto T. Induction of brain-derived neurotrophic factor (BDNF) and the receptor trk B mRNA following middle cerebral artery occlusion in rat. *Neurosci Lett*. 1996;211:57–60.
5. Kitagawa H, Sasaki C, Zhang WR, Sakai K, Shiro Y, Wanita H, Matsumoto Y, Mori T, Abe K. Induction of glial cell line-derived neurotrophic factor receptor proteins in cerebral cortex and striatum after permanent middle cerebral artery occlusion in rats. *Brain Res*. 1999;834:190–195.
6. Lennmyr F, Ata KA, Funa K, Olsson Y, Terent A. Expression of vascular endothelial growth factor (VEGF) and its receptors (Flt-1 and Flk-1) following permanent and transient occlusion of the middle cerebral artery in the rat. *J Neuropathol Exp Neurol*. 1998;57:874–882.
7. Hayashi T, Abe K, Sakurai M, Itoyama Y. Inductions of hepatocyte growth factor and its activator in rat brain with permanent middle cerebral artery occlusion. *Brain Res*. 1998;799:311–316.
8. Hayashi T, Abe K, Itoyama Y. Reduction of ischemic damage by application of vascular endothelial growth factor in rat brain after transient ischemia. *J Cereb Blood Flow Metab*. 1998;18:887–895.
9. Shimamura M, Iwase M, Fujikawa S, Washizawa K, Kotsuka S, Maeda M, Watabe K, Yoshikawa Y, Hasegawa M. Postischemic administration of Sendai virus vector carrying neurotrophic factor genes prevents delayed neuronal death in gerbils. *Gene Ther*. 2004;11:784–790.
10. Shimamura M, Sato N, Oshima K, Aoki M, Kurinami H, Waguri S, Uchiyama Y, Ogihara T, Kaneda Y, Morishita R. Novel therapeutic strategy to treat brain ischemia: overexpression of hepatocyte growth factor gene reduced ischemic injury without cerebral edema in rat model. *Circulation*. 2004;109:424–431.
11. Date I, Takagi N, Takagi K, Kago T, Matsumoto K, Nakamura T, Takeo S. Hepatocyte growth factor attenuates cerebral ischemia-induced learning dysfunction. *Biochem Biophys Res Commun*. 2004;319:1152–1158.
12. Zhang WR, Sato K, Iwai M, Nagano I, Manabe Y, Abe K. Therapeutic time window of adenovirus-mediated GDNF gene transfer after transient middle cerebral artery occlusion in rat. *Brain Res*. 2002;947:140–145.
13. Nagayama T, Nagayama M, Kohara S, Kamiguchi H, Shibuya M, Katoh Y, Itoh J, Shinohara Y. Post-ischemic delayed expression of hepatocyte growth factor and c-Met in mouse brain following focal cerebral ischemia. *Brain Res*. 2004;999:155–166.
14. Kovacs Z, Ikezaki K, Samoto K, Inamura T, Fukui M. VEGF and flt. Expression time kinetics in rat brain infarct. *Stroke*. 1996;27:1865–1873.
15. Nakamura T, Nawa K, Ichihara A. Partial purification and characterization of hepatocyte growth factor from serum of hepatectomized rats. *Biochem Biophys Res Commun*. 1984;122:1450–1459.
16. Nakamura T, Nishizawa T, Hagiya M, Seki T, Shimonishi M, Sugimura A, Tashiro K, Shimizu S. Molecular cloning and expression of human hepatocyte growth factor. *Nature*. 1989;342:440–443.
17. Honda S, Kagoshima M, Wanaka A, Tohyama M, Matsumoto K, Nakamura T. Localization and functional coupling of HGF and c-Met/HGF receptor in rat brain: implication as neurotrophic factor. *Brain Res Mol Brain Res*. 1995;32:197–210.
18. Sun W, Funakoshi H, Nakamura T. Localization and functional role of hepatocyte growth factor (HGF) and its receptor c-met in the rat developing cerebral cortex. *Brain Res Mol Brain Res*. 2002;103:36–48.
19. Kokuzawa J, Yoshimura S, Kitajima H, Shimoda J, Kaku Y, Iwama T, Morishita R, Shimazaki T, Okano H, Kunisada T, Sakai N. Hepatocyte growth factor promotes proliferation and neuronal differentiation of neural stem cells from mouse embryos. *Mol Cell Neurosci*. 2003;24:190–197.
20. Miyazawa T, Matsumoto K, Ohmichi H, Katoh H, Yamashima T, Nakamura T. Protection of hippocampal neurons from ischemia induced delayed neuronal death by hepatocyte growth factor: a novel neurotrophic factor. *J Cereb Blood Flow Metab*. 1998;18:345–348.
21. Yoshimura S, Morishita R, Hayashi K, Kokuzawa J, Aoki M, Matsumoto K, Nakamura T, Ogihara T, Sakai N, Kaneda Y. Gene transfer of hepatocyte growth factor to subarachnoid space in cerebral hypoperfusion model. *Hypertension*. 2002;39:1028–1034.
22. Hayashi K, Morishita R, Nakagami H, Yoshimura S, Hara Y, Matsumoto K, Nakamura T, Ogihara T, Kaneda Y, Sakai N. Gene therapy for

preventing neuronal death using hepatocyte growth factor: in vivo gene transfer of HGF to subarachnoid space prevents delayed neuronal death in gerbil hippocampal CA1 neurons. *Gene Ther*. 2001;8:1167–1173.

23. Tsuzuki N, Miyazawa T, Matsumoto K, Nakamura T, Shiota K, Chigasaki H. Hepatocyte growth factor reduces infarct volume after transient focal cerebral ischemia in rats. *Acta Neurochir Suppl*. 2000;76:311–316.

24. Kaneda Y, Nakajima T, Nishikawa T, Yamamoto S, Ikegami H, Suzuki N, Nakamura H, Morishita R, Kohno H. Hemagglutinating virus of Japan (HVJ) envelope vector as a versatile gene delivery system. *Mol Ther*. 2002;6:219–226.

25. Shimamura M, Morishita R, Endoh M, Oshima K, Aoki M, Waguri S, Uchiyama Y, Kaneda Y. HVJ envelope vector for gene transfer into central nervous system. *Biochem Biophys Res Commun*. 2003;300:362–371.

26. Koike H, Morishita R, Iguchi S, Aoki M, Matsumoto K, Nakamura T, Yokoyama C, Tanabe T, Ogihara T, Kaneda Y. Enhanced angiogenesis and improvement of neuropathy by coinjection of human hepatocyte growth factor and prostacyclin synthase gene. *Lasch J*. 2003;17:779–781.

27. Petullo D, Masonic K, Lincoln C, Wubbenley L, Telska M, Yao DL. Model development and behavioral assessment of focal cerebral ischemia in rats. *Life Sci*. 1999;62:1099–1105.

28. Modo M, Stroemer RP, Tang E, Veizovic T, Sowniski P, Hodges H. Neurological sequelae and long-term behavioural assessment of rats with transient middle cerebral artery occlusion. *J Neurosci Methods*. 2000;104:99–109.

29. Chen J, Zhang C, Jiang H, Li Y, Zhang L, Robin A, Katakowski M, Lu M, Chopp M. Atorvastatin induction of VEGF and BDNF promotes brain plasticity after stroke in mice. *J Cereb Blood Flow Metab*. 2005;25:281–290.

30. Nedergaard M, Gjedde A, Diemer NH. Hyperglycaemia protects against neuronal injury around experimental brain infarcts. *Neurol Res*. 1987;9:241–244.

31. Takamatsu H, Tatsumi M, Nitta S, Ichise R, Muramatsu K, Iida M, Nishimura S, Umemura K. Time courses of progress to the chronic stage of middle cerebral artery occlusion models in rats. *Exp Brain Res*. 2002;146:95–102.

32. DeVries AC, Nelson RJ, Traystman RJ, Hurn PD. Cognitive and behavioral assessment in experimental stroke research: will it prove useful? *Neurosci Biobehav Rev*. 2001;25:325–342.

33. Robinson RG. Differential behavioral and biochemical effects of right and left hemispheric cerebral infarction in the rat. *Science*. 1979;205:707–710.

34. O'Kane EM, Stone TW, Morris BJ. Distribution of Rho family GTPases in the adult rat hippocampus and cerebellum. *Brain Res Mol Brain Res*. 2003;114:1–8.

35. Schabitz WR, Berger C, Kollmar R, Seitz M, Tanay E, Kiessling M, Schwab S, Sommer C. Effect of brain-derived neurotrophic factor treatment and forced arm use on functional motor recovery after small cortical ischemia. *Stroke*. 2004;35:992–997.

36. Stroemer RP, Kent TA, Hulsebosch CE. Enhanced neocortical neural sprouting, synaptogenesis, and behavioral recovery with D-amphetamine therapy after neocortical infarction in rats. *Stroke*. 1998;29:2381–2395.

37. Albrecht PJ, Murtie JC, Ness JK, Redwine JM, Enterline JR, Armstrong RC, Levison SW. Astrocytes produce CNTF during the remyelination phase of viral-induced spinal cord demyelination to stimulate FGF-2 production. *Neurobiol Dis*. 2003;13:89–101.

38. Tada T, Nguyen JB, Hitoshi Y, Watson NP, Dunn JF, Ohara S, Nagano S, Kosai K, Israel MA. Diffuse encephaloventriculitis and substantial leukoencephalopathy after intraventricular administration of recombinant adenovirus. *Neurol Res*. 2005;27:378–386.

39. Maina F, Klein R. Hepatocyte growth factor, a versatile signal for developing neurons. *Nat Neurosci*. 1999;2:213–217.

40. Modo M, Stroemer RP, Tang E, Patel S, Hodges H. Effects of implantation site of stem cell grafts on behavioral recovery from stroke damage. *Stroke*. 2002;33:2270–2278.

41. Casu MA, Wong TP, De Koninck Y, Ribeiro-da-Silva A, Cuello AC. Aging causes a preferential loss of cholinergic innervation of characterized neocortical pyramidal neurons. *Cereb Cortex*. 2002;12:329–337.

42. Olenik C, Barth H, Just I, Aktories K, Meyer DK. Gene expression of the small GTP-binding proteins RhoA, RhoB, Rac1, and Cdc42 in adult rat brain. *Brain Res Mol Brain Res*. 1997;52:263–269.

43. Royal I, Lamarche-Vane N, Lamorte L, Kaibuchi K, Park M. Activation of cdc42, rac, PAK, and rho-kinase in response to hepatocyte growth factor differentially regulates epithelial cell colony spreading and dissociation. *Mol Biol Cell*. 2000;11:1709–1725.

44. Kornack DR, Rakic P. Cell proliferation without neurogenesis in adult primate neocortex. *Science*. 2001;294:2127–2130.

45. Rakic P. Adult neurogenesis in mammals: an identity crisis. *J Neurosci*. 2002;22:614–618.

46. Jiang W, Gu W, Brannstrom T, Rosqvist R, Wester P. Cortical neurogenesis in adult rats after transient middle cerebral artery occlusion. *Stroke*. 2001;32:1201–1207.

47. Zhang RL, Zhang ZG, Zhang L, Chopp M. Proliferation and differentiation of progenitor cells in the cortex and the subventricular zone in the adult rat after focal cerebral ischemia. *Neuroscience*. 2001;105:33–41.

48. Shimazaki K, Yoshida K, Hirose Y, Ishimori H, Katayama M, Kawase T. Cytokines regulate c-Met expression in cultured astrocytes. *Brain Res*. 2003;962:105–110.

49. Wei L, Erinjeri JP, Rovainen CM, Woolsey TA. Collateral growth and angiogenesis around cortical stroke. *Stroke*. 2001;32:2179–2184.

50. Alexandrov AV, Hall CE, Labiche LA, Wozniak AW, Grotta JC. Ischemic stunning of the brain: early recanalization without immediate clinical improvement in acute ischemic stroke. *Stroke*. 2004;35:2320–2325.

51. Van Bruggen N, Thibodeaux H, Palmer JT, Lee WP, Fu L, Cairns B, Tumas D, Gerlai R, Williams SP, Van Bruggen N, Eastham-Anderson J, French D, Peale FV, Carano RA, Wu AY, Kasman I, Cheng Z, Ross J, Ferrara N. VEGF antagonism reduces edema formation and tissue damage after ischemia/reperfusion injury in the mouse brain. *J Clin Invest*. 1999;104:1613–1620.

52. Hamanoue M, Takemoto N, Matsumoto K, Nakamura T, Nakajima K, Kohsaka S. Neurotrophic effect of hepatocyte growth factor on central nervous system neurons in vitro. *J Neurosci Res*. 1996;43:554–564.

53. Oshima K, Shimamura M, Mizuno S, Tamai K, Doi K, Morishita R, Nakamura T, Kubo T, Kaneda Y. Intrathecal injection of HVJ-E containing HGF gene to cerebrospinal fluid can prevent and ameliorate hearing impairment in rats. *Lasch J*. 2004;18:212–214.

科学評論社「神経内科」第65巻第2号(2006年8月)
特集／拡散テンソルに基づくMRI画像の進歩

題名

3. 大脳皮質・深部灰白質間の線維連絡

Connectivity between cerebral cortex and deep gray matter

著者
林　拓也[1,2]
Takuya Hayashi, MD, PhD

所属
[1]国立循環器病センター研究所放射線医学部, National Cardiovascular Center, Research Institute, Department of Investigative Radiology
[2]モントリオール神経研究所脳画像研究部門, Montreal Neurological Institute, Brain Imaging Center

Key Words: diffusion tensor, tractography, striatum, thalamus

1. はじめに

近年の拡散テンソルMRI（DTI）法の撮像・解析技術の進歩により、脳内の拡散移動度の評価およびそれに基づく脳内の巨視的線維連絡性の評価（diffusion-based tractography）が可能になり、ヒト中枢神経疾患の病態や脳内線維連絡性の解明に貢献すると期待されている。本稿では特にdiffusion-based tractographyに関した近年の技術進歩と大脳皮質－深部灰白質間の線維連絡解明の応用研究を紹介し、神経内科領域における臨床検査への応用性について考えてみたい。

2. 脳の拡散異方性からDTI、DTIからtractographyへ

Diffusion-based tractographyはそもそも脳内の水分子の拡散運動(diffusion)が空間的に均等（等方性isotropic）でないという特殊な物理的性質のために可能となった技術である。なぜ神経系で拡散が等方性でない（逆は異方性anisotropicと呼ぶ）のか未解明な部分も多いがいくつか面白い研究がある。当初神経系にのみ存在し電気絶縁体として働く髄鞘（ミエリン）が疑われたがBeaulieuらはダツという鼻の長い魚の嗅球神経および三叉神経（御存知の通り、前者は無髄神経、後者は有髄神経の束である）の拡散異方性を調べたところ、どちらも同じ程度の異方性であった（すなわち神経線維走行の方向には拡散しやすく、垂直方向には拡散が制限されていたがその相対比は同程度だった）[(1)]（図1）。また彼らは、（拡散よりも大きな動きである）軸索流を阻害する薬(vinblastine：微小管の機能を抑制する)を用いたり、軸索膜の寄与の少ないヤリイカ巨大神経を使って、軸索流の影響や、軸索内長軸方向の蛋白構造物(microtubuleなど)の影響を検討したがいずれも異方性に寄与しなかった[(1)]。その後、他の研究者が髄鞘形成前の新生仔ラットや遺伝性髄鞘欠損ラットの脳でも強い異方性を観察したことから、主に軸索膜、次に髄鞘膜が拡散異方性の原因と考えられている（総説[(1)]参照）。

Diffusion tensor imaging(DTI)法は、motion probing gradient, MPG[†]という傾斜磁場を均等に多方向（最低6方向）で用いることで相対的拡散移動度の空間的特徴をdiffusion tensorとして表現し画像化する方法である[(2)]。MPGには方向性があり、MPGと同じ方向の拡散運動が大きい部位で信号が低下する。たとえば左右方向にMPGをかけると脳梁の部分の信号が低下し、上下方向にかけると内包の部分の信号が低下する。脳内のある一点に注目すると、その部分の水分子が全く自由に拡散する等方性の状態であれば、原点からの水分子の相対的移動は球になる。一方、方向依存性に拡散が制限される場合（異方性anisotropic）には楕円体になる[‡]。この楕円体又は球の形で表される水分子の相対的拡散移動度は数学的概念で

---

† 1965年にStejskal & Tannerが開発した拡散を強調するための傾斜磁場。その後1986年にLeBihanらが医学領域への応用性を紹介して以後diffusion MRIの医学研究が進んだ。特に急性期脳梗塞で強い拡散の変化が生じることが発見され、エコープラナーイメージングEPI法と組み合わせて高速撮像が可能となったことで臨床用MRI装置への導入が進んだ。

‡ このtensor modelは非常に単純なモデルで、拡散の均一性と線形性を仮定しているため

ある tensor で表現することができ、異なる MPG 方向の複数の拡散強調 MRI データから画素毎に計算することができる。この楕円体の最も長い軸方向（第一固有ベクトル principal eigenvector）は同画素内で支配的に存在する神経線維方向に一致すると考えられる(図 2C)。これを隣の画素同志たどっていくのが神経線維追跡法(diffusion-based tractography)であり、この方法の開発には日本人研究者の貢献が大きく Johns Hopkins 大学の森進教授の方法はこの研究分野を拡大した[3]。

しかし diffusion-based tractography は、データ収集・解析法自体に未だ議論が多くその精度の検証に至っていない。当然精度高い tensor の推定のために、より方向数の多い MPG によって角度解像度の高い画像収集が望まれている。また解析の問題として、tracking 途中に等方性の tensor に遭遇したとき（すなわち形が球に近いとき）にその主軸方向が推定できず tracking がそれ以上先に進められなかった。そのため単一方向の線維を支配的に含むような領域（脳梁、錐体路、視放線など）の線維連絡性の評価はできても、線維が交差するような場所や灰白質内の線維連絡性の評価は困難であった。

こうした解析の問題を克服するべく多くの研究が進められており、各画素における各方向の拡散移動を tensor ではなく確率分布として表現する方法や、従来の tensor model に代わり非線形拡散を考慮した方法[§]が提唱されている。前者は、各画素における各方向への拡散移動の確率分布(*pdf*)を、ベイズの定理および bootstrap 法と呼ばれるサンプリング法によって評価しそれに基づいて確率的に線維連絡を評価する(diffusion-weighted probabilistic tractography) [4]。すなわち従来の方法では画素の間の線維連絡性が繋がるか繋がらないかのバイナリーであったのに対しこの probabilistic tractography では確率として表現したことで線維追跡能を格段に向上させ定量的な評価を可能にした。

次項ではこの方法により明らかにされてきた大脳皮質と深部灰白質の線維連絡性について述べる。

3．大脳皮質・深部灰白質間の神経線維連絡

ヒト脳の巨視的な神経線維連絡性の知識はほとんどサル（主にマカク属）脳での神経線維トレーサー（放射能標識アミノ酸、西洋ワサビ過酸化酵素など）によって得られた知見から推定されてきた。ただヒトの巨視的線維連絡性の評価法が今まで全く無かったわけではなく、Klingler 法という方法があった[5]。これは神経解剖の教科書でもよく見るもので、

に単純な形状（楕円体）になる。

[§]前述のように従来の tensor model は線形性・均一性を仮定していたが、特定の拡散モデルを仮定せず画素内の交差線維を推定する q-ball 法[4]、画素内の拡散運動の非線形性を考慮した generalized diffusion tensor model 法[5]、q-ball と確率的線維連絡追跡法の混合モデル[6]、等が提唱されている。

剖検脳をまるごとゆっくりと凍結・解凍を繰り返すことで脳組織内の氷の結晶を伸長させ脳内の線維方向に沿った方向に dissection しやすくするものである。この手法によってヒト脳の脳梁、視放線、錐体路、放線冠、鉤状・弓状束、上・下縦束といった主要な線維束を肉眼的に可視化することができる**（図 2B）。しかしこの手法は dissection 自体に技術と経験を要し、その結果も定量的でない††。

さて大脳深部灰白質のうち間脳から発生した「視床」は、脳幹、脊髄、小脳、大脳基底核からの入力を中継し大脳皮質に出力する核である。ヒト剖検脳での組織化学による細胞構築や化学的性質とサル脳での細胞構築・線維連絡性の対応によってかなり視床内核の境界・構造が詳細にわかっている[6]。また視床内核毎に大脳皮質との線維連絡性が明確に異なることも知られている。Behrens ら[7]は diffusion-weighted probabilistic tractography によってヒトの視床を線維連絡性にもとづいて分節化することに成功し、この結果が従来知られていた視床内分節化とよく一致した（図 4A）。また同時に外側膝状体から視覚野へ行く視放線のみならず、視床内側核と前頭前野や側頭葉内側部への線維連絡、視床腹外側核と運動感覚野の線維連絡等も示した（図 3A-D）。また彼らは、この方法によって、脳画像領域で一般に用いられるヒト標準脳空間（モントリオール神経研究所 MNI テンプレート）の視床内の各 voxel の大脳皮質との連絡性およびそれに基づく視床内核のアトラスを作成した（図 4C）。しかし、最近のサル脳の研究で皮質から視床への逆行性線維が発見され注目されている[8]が、残念ながら現存の diffusion-based tractography で線維連絡の方向性（神経細胞→軸索末端又は軸索末端→神経細胞）はわからない。

大脳深部灰白質のうち大脳皮質と同じく終脳から発生した「大脳基底核」は運動、認知、感情、報酬、学習、言語など様々な脳機能に関連する重要な脳部位である。そのうち線条体は神経内科領域でもパーキンソン病やハンチントン病をはじめとする多くの変性疾患の病態に関与する馴染みある部位である。線条体は被殻と尾状核に分かれるが発生学的に同じ構造物であり、細胞構築も比較的均一で組織化学による染色でも明確な線条体内の境界は認められない。損傷・疾患脳の観察で、特定の神経脱落症状が出現する場合もあるが、何も症状を示さないこともあり機能の局在化が難しい。そのためか古くからサル脳によるトレーサー研究で大脳皮質との連絡性に基づいた線条体内のマッピングを行った研究が多く、それらの観察から大脳皮質－大脳基底核－視床－大脳皮質から成る神経回路（ループ）に関連したモデルも提唱された。

** 実際の dissection の様子をビデオで見ることが出来る（アメリカ脳神経外科学会の website : http://www.aans.org/education/journal/neurosurgical/June05/18-6b-4.pdf 内に教育用ビデオのリンクがある）

†† その他 Nauta 法のように損傷脳の剖検脳を用いて、変性した軸索を染色・検索することで損傷部位との線維連絡性を調べる方法や、カルボシアニン色素による剖検脳での線維連絡性評価もあるが、観察機会が限られたり、短い距離の線維連絡しか評価できない。